

# Heat Conduction in the Vortex State of $\text{NbSe}_2$ : Evidence for Multi-Band Superconductivity

Etienne Boaknin,<sup>1</sup> M.A. Tanatar,<sup>1</sup> Johnpierre Paglione,<sup>1</sup> D. Hawthorn,<sup>1</sup> F. Ronning,<sup>1</sup> R.W. Hill,<sup>1</sup> M. Sutherland,<sup>1</sup> Louis Taillefer,<sup>1,2</sup> Jeff Sonier,<sup>2,3</sup> S.M. Hayden,<sup>4</sup> and J.W. Brill<sup>5</sup>

<sup>1</sup>*Department of Physics, University of Toronto, Toronto, Ontario, Canada*

<sup>2</sup>*Canadian Institute for Advanced Research, Toronto, Ontario, Canada*

<sup>3</sup>*Simon Fraser University, Department of Physics, Burnaby, Canada*

<sup>4</sup>*H. H. Wills Physics Laboratory, University of Bristol, Bristol BS8 1TL, United Kingdom*

<sup>5</sup>*Department of Physics and Astronomy, University of Kentucky, Lexington, Kentucky, 40506-0055*

(Dated: May 21, 2019)

The thermal conductivity  $\kappa$  of the layered  $s$ -wave superconductor  $\text{NbSe}_2$  was measured down to  $T_c/100$  throughout the vortex state. The electronic contribution  $\kappa/T$  as  $T \rightarrow 0$  is found to be zero in zero magnetic field, as expected for a fully-gapped Fermi surface. With increasing field, we identify two regimes: one with localized states at fields very near  $H_{c1}$  and one with highly delocalized quasiparticle excitations at higher fields. The two associated length scales are most naturally explained as multi-band superconductivity, with distinct small and large superconducting gaps on different sheets of the Fermi surface. This behaviour is compared and contrasted to those of the multi-band superconductor  $\text{MgB}_2$  and the conventional superconductor  $\text{V}_3\text{Si}$ .

PACS numbers: 74.70.Ad, 74.25.Fy, 74.25.Qt, 74.25.Jb

Multi-band superconductivity (MBSC) is the existence of a superconducting gap of significantly different magnitude on distinct parts (sheets) of the Fermi surface. This unusual phenomenon has recently emerged as a possible explanation for the anomalous properties of some  $s$ -wave superconductors. Although the first experimental observation of MBSC was reported twenty years ago [1], the possibility of MBSC has not often been raised since then. The current interest has been fuelled by the peculiar properties of the 40-K superconductor  $\text{MgB}_2$ , where the case for MBSC is now rather compelling [2]. In particular, a gap much smaller than the expected BCS gap (of order  $2k_B T_c$ ) has been resolved in tunneling experiments [3]. A consequence of this small gap is the much more rapid excitation of quasiparticles than usual, which can make the properties of this  $s$ -wave superconductor similar to those of  $d$ -wave superconductors, for example.

Based on angle-resolved photoemission (ARPES) measurements, it has recently been proposed that the 7-K layered superconductor  $\text{NbSe}_2$  is also host to MBSC [4]. They reveal a sizable difference in the magnitude of the superconducting gap on the two sets of Fermi surface (FS) sheets, with no observed gap on the smallest sheet. However, these measurements were only performed at 5.3 K. It is clearly of interest to shed further light on this sheet-dependent superconductivity by performing bulk measurements down to very low temperature.

In this Letter, we report a study of heat transport in  $\text{NbSe}_2$  at very low temperatures throughout the vortex state, providing further evidence for MBSC. By measuring the degree of delocalization of quasiparticle states in the vortex state, heat transport probes the overlap between core states on adjacent vortices, *i.e.* the size of the vortex core ( $\sim \xi$ ), and hence the magnitude of the gap

( $\sim 1/\xi$ ). We resolve two regimes of behaviour: one limited to very low fields (up to  $\sim 5H_{c1}$ ), where delocalization is slow and activated as in conventional (single-gap) superconductors like  $\text{V}_3\text{Si}$ , and one for all other fields up to  $H_{c2}$  where quasiparticles transport heat extremely well, as in unconventional superconductors with nodes in the gap. Note that in the case of  $\text{NbSe}_2$  the absence of any residual linear term in the thermal conductivity confirms that there are no nodes in the gap.

$\text{NbSe}_2$  is a layered quasi-2D metal with hexagonal symmetry. It displays a transition to a charge density wave state around  $T \simeq 35$  K. Its Fermi surface has been measured at low temperatures by both de Haas-van Alphen (dHvA) [5] and ARPES measurements [4]. These agree with band structure calculations which derive a FS made of a number of sheets (4 or 5). These sheets divide into two groups: a small  $\Gamma$ -centered pocket derived from the Se  $4p$  band (denoted as  $\Gamma$  band from now on) and larger more two-dimensional sheets derived from Nb  $3d$  bands. Superconductivity sets in at  $T_c = 7$  K. Tunneling spectroscopy at 50 mK reveals a spectrum that is flat at low voltage but not of the ideal BCS shape. Rather, it is consistent with a distribution of gaps that range from 0.7 to 1.4 meV [6]. In the vortex state at very low fields (near  $H_{c1}$ ), a zero-bias conductance peak characteristic of states localized in the vortex core is observed at the vortex centre.

The thermal conductivity  $\kappa$  of  $\text{NbSe}_2$  was measured in a dilution refrigerator using a standard steady-state technique [7]. The measurements were made at temperatures increasing from 50 mK and in magnetic fields ranging from 0 to 6 T, applied parallel to the  $c$ -axis of the hexagonal crystal structure, and perpendicular to the heat current (in the plane). The sample was cooled in

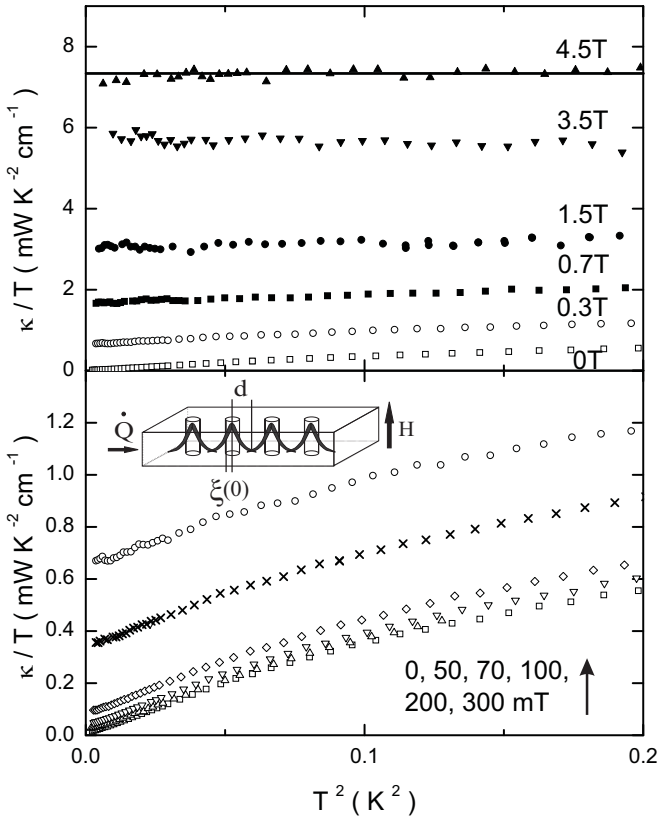


FIG. 1: Temperature dependence of thermal conductivity in NbSe<sub>2</sub> at several applied fields, plotted as  $\kappa/T$  vs  $T^2$ . The solid line indicates the value expected from the Wiedemann-Franz law as obtained from resistivity measurements at  $H = 4.5$  T. The field is applied parallel to the  $c$ -axis and perpendicular to the heat current  $Q$ .

field to ensure field homogeneity. The thermal conductivity was also measured as a function of field at fixed temperature resulting in nearly no difference as compared to the field-cooled data.

The sample is from the same batch as the one used by Sonier *et al.* [8, 9] and has a superconducting transition temperature  $T_c = 7.0$  K with a width  $\delta T_c = 0.1$  K. The residual resistivity ratio is 40, with a residual resistivity of  $\rho_0 \simeq 3 \mu\Omega \text{ cm}$ . The upper and lower critical fields are respectively  $H_{c2} = 4.5$  T and  $H_{c1} = 20$  mT for  $H \parallel c$ . The coherence length estimated from  $H_{c2}$  is  $\xi(0) = 85$  Å. The sample is in the clean limit with a ratio of the BCS coherence length  $\xi_0$  to the mean free path  $l$  in the plane being  $\xi_0/l \simeq 0.15$  [10]. The sample was a rectangular parallelepiped with dimensions  $1.2 \times 0.5$  mm in the plane, and 0.1 mm along the  $c$ -axis. It was cleaved to provide six fresh surfaces for contacts. These were made shortly after with Dupont 4929N silver paint to give contact resistances of roughly  $20 \text{ m}\Omega$  at low temperatures.

The thermal conductivity of NbSe<sub>2</sub> is plotted in Fig. 1, as  $\kappa/T$  against  $T^2$ . This enables a separation between the electronic and the phononic thermal conductivity since

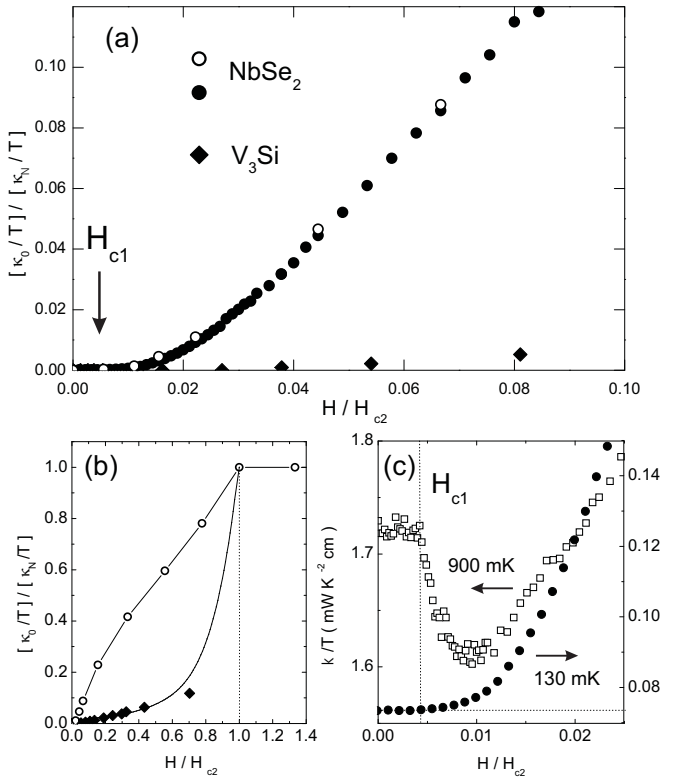


FIG. 2: (a,b) Thermal conductivity of NbSe<sub>2</sub> (empty circles) and V<sub>3</sub>Si (diamonds) at  $T \rightarrow 0$  vs  $H$ , normalized to values at  $H_{c2}$ . The filled circles come from a sweep in field at  $T = 130$  mK from which the value of the  $H = 0$  thermal conductivity (the phononic contribution) has been subtracted. The thick solid line in (b) is a theoretical curve for the thermal conductivity of V<sub>3</sub>Si [13]. The other (thin) line is a guide to the eye. (c)  $\kappa/T$  vs  $H$  for NbSe<sub>2</sub> at  $T = 130$  mK (circles) and  $T = 900$  mK (squares). The latter shows a typical drop in the phononic thermal conductivity at  $H_{c1} = 20$  mT. The former shows that the electronic thermal conductivity starts to increase right at  $H_{c1}$  but has a slow activated-like behavior for fields below  $0.03 H_{c2}$ .

the asymptotic dependence of the former as  $T \rightarrow 0$  is linear in  $T$  while that of the latter is cubic. The electronic thermal conductivity is thus obtained as the extrapolated  $T \rightarrow 0$  value labelled  $\kappa_0/T$ . In zero field,  $\kappa_0/T = 0.000 \pm 0.005 \text{ mW K}^{-2} \text{ cm}^{-1}$ , so that the thermal conductivity is purely phononic. This is a clear indication that NbSe<sub>2</sub> is an *s*-wave superconductor where the excitation spectrum is fully gapped. However, as soon as a magnetic field is applied, an electronic contribution develops as a rigid shift from the  $H = 0$  curve in Fig. 1. At higher fields, the electronic contribution dominates the conduction and  $\kappa/T$  is constant in temperature. Above  $H_{c2}$ , the Wiedemann-Franz law is satisfied and the thermal conductivity saturates.

The  $\kappa_0/T$  values are plotted as a function of  $H$  on a reduced scale in Fig. 2. Also plotted is a field sweep at  $T = 130$  mK from which the zero-field value (the

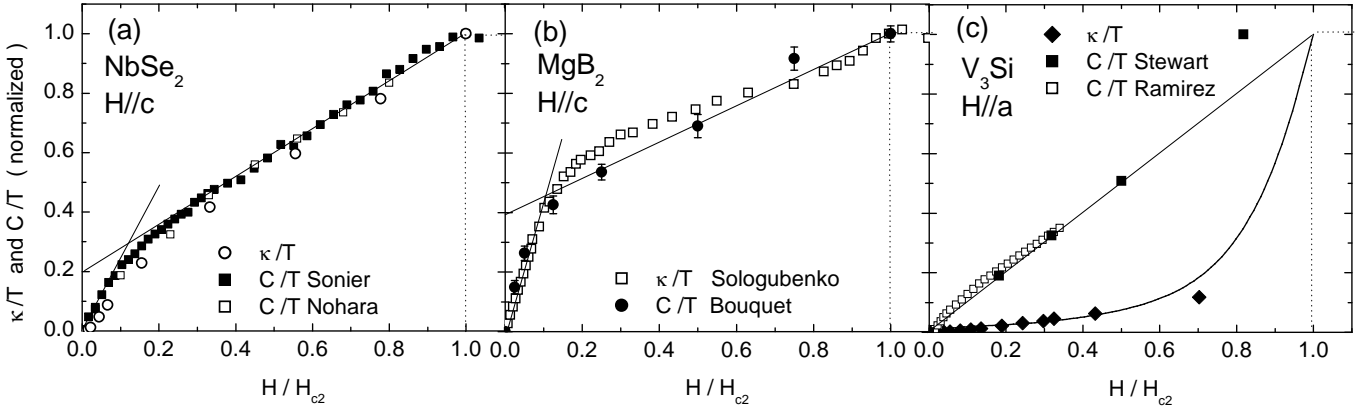


FIG. 3: (a) Thermal conductivity and heat capacity of  $\text{NbSe}_2$  normalized to the normal state value vs  $H/H_{c2}$ . The heat capacity was measured in two different ways: i) at  $T = 2.4$  K on the same crystals as used in this study [8], and ii) extrapolated to  $T \rightarrow 0$  from various temperature sweeps on different crystals [16]. (b) Equivalent data for  $\text{MgB}_2$  single crystals [17, 18]. (c) Equivalent data for  $\text{V}_3\text{Si}$ , with a theoretical curve for  $\kappa/T$  [13]. The specific heat is measured at  $T = 3.5$  K [19] and extrapolated to  $T = 0$  [20]. The straight line is a linear fit. The thermal conductivity is seen to follow very closely the specific heat for both  $\text{NbSe}_2$  and the multiband superconductor  $\text{MgB}_2$ . It does not, however, for the conventional *s*-wave superconductor  $\text{V}_3\text{Si}$ .

phononic contribution) has been subtracted. As seen in Fig. 2c, the thermal conductivity starts to increase right at  $H_{c1}$  in what could be qualified as an activated behavior, although in a very limited range of fields:  $H_{c1} \leq H \leq 0.03H_{c2}$ . The value of  $H_{c1}$  is determined in situ as the drop in the phonon  $\kappa$  due to vortex scattering. At higher fields ( $H > 0.03H_{c2}$ ),  $\kappa_0/T$  increases rapidly, *i.e.* faster than  $(H/H_{c2}) \kappa_N/T$ , where  $\kappa_N/T$  is the normal state value. This shows the presence of *highly delocalized quasiparticle states almost throughout the vortex state of  $\text{NbSe}_2$* .

This is in stark contrast to the behavior expected of a type-II *s*-wave superconductor. Indeed, when a field in excess of  $H_{c1}$  is applied, and vortices enter the sample, the conventional picture is that the induced electronic states are *localized* within the vortex cores. As one increases the field, the intervortex spacing  $d \simeq \sqrt{\Phi_0/B}$  decreases, in the same way for all type-II superconductors. The localized states in adjacent vortices will have an increasing overlap leading to enhanced tunneling between vortices. In other words, bands of conduction are formed. Strictly speaking, the electronic states are actually always delocalized but with extremely flat bands at low fields [11]. As these get gradually more dispersive, the thermal conductivity should increase accordingly and grow exponentially with the ratio  $d/\xi$ . This exponential behavior is indeed observed in Nb where the conduction is activated as a function of field [12].

A better point of comparison for  $\text{NbSe}_2$  is  $\text{V}_3\text{Si}$ , another extreme type-II superconductor with similar superconducting parameters ( $T_c = 17$  K,  $\xi = 50$  Å). This is done in Fig. 2, where the thermal conductivity of  $\text{V}_3\text{Si}$  is seen to grow much more slowly with  $H$  than that of  $\text{NbSe}_2$ , and is well described by theory [13]. Quantitatively, at  $H = H_{c2}/20$ ,  $\kappa_0/T = \frac{1}{20} \times \kappa_N/T$  for  $\text{NbSe}_2$

and  $\frac{1}{400} \times \kappa_N/T$  for  $\text{V}_3\text{Si}$  [14]. Note that the samples compared in Fig. 2 are in the same purity regime. From the standard relation  $\xi(0) = 0.74\xi_0[\chi(0.88\xi_0/l)]$ , where  $\chi$  is the Gor'kov function (equal to unity in the clean limit), we obtain for  $\text{V}_3\text{Si}$   $\xi_0/l = 0.13$ , with values of  $\xi(0) = 50$  Å coming from  $H_{c2}$  and  $l = 1500$  Å from dHvA measurements [15]. This is similar to the value of 0.15 for  $\text{NbSe}_2$ .

The high level of delocalization in  $\text{NbSe}_2$  is a clear indication of either a gap with nodes (*e.g.* *d*-wave) or a nodeless gap which is either highly anisotropic or small on one FS and large on another. A gap with nodes is ruled out by the absence of a residual term in the thermal conductivity in zero field.

It is revealing to compare  $\text{NbSe}_2$  to  $\text{MgB}_2$  for which the thermal conductivity has a similar field dependence. Strikingly, the thermal conductivity follows roughly the same field dependence as the specific heat for  $\text{NbSe}_2$  and  $\text{MgB}_2$  for most of the field range. This is shown in Fig. 3 where the thermal conductivity  $\kappa(H)$  and the specific heat  $C(H)$  normalized to their normal state values are plotted on a reduced field scale for single crystals of  $\text{NbSe}_2$  [8, 16],  $\text{MgB}_2$  [17, 18], and  $\text{V}_3\text{Si}$  [19, 20], for magnetic fields along the *c*-axis for hexagonal  $\text{NbSe}_2$  and  $\text{MgB}_2$ , and along the *a*-axis for cubic  $\text{V}_3\text{Si}$ . In conventional superconductors like  $\text{V}_3\text{Si}$ ,  $\kappa(H)$  and  $C(H)$  are very different (see Fig. 3c), because the excited electronic states are largely localized.

$\text{MgB}_2$  is a well established case of MBSC with a small gap on one FS ( $\Delta_\pi = 1.8$  meV) and a large gap on the other ( $\Delta_\sigma = 6.8$  meV). The field dependence of its heat capacity is well understood in this context [18], with a distinctive shoulder at a field of  $H_{c2}/10$  (see Fig. 3b). A similar shoulder is also manifest in  $\text{NbSe}_2$  around  $H_{c2}/8$  (see Fig. 3a). Empirically, the striking fact that heat

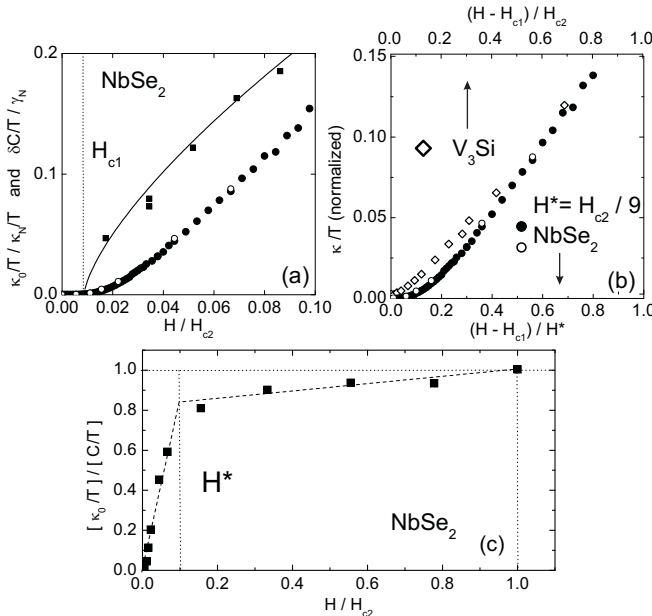


FIG. 4: (a) Thermal conductivity (circles) and heat capacity (squares) [8] of  $\text{NbSe}_2$  normalized to the normal state values vs  $H/H_{c2}$  at very low fields. The line is a guide to the eye. (b) Normalized thermal conductivity of  $\text{NbSe}_2$  vs  $(H - H_{c1})/H^*$  (with  $H^* = 9 H_{c2}$ ) and  $\text{V}_3\text{Si}$  vs  $(H - H_{c1})/H_{c2}$ . (c) Ratio of heat transport to heat capacity in  $\text{NbSe}_2$ , a measure of the degree of delocalization.

transport and heat capacity have the same field dependence in both materials points to a common explanation, and hence suggests that  $\text{NbSe}_2$  is host to multi-band superconductivity [23]. This is consistent with recent ARPES measurements at  $T = 0.8 T_c$  which resolved a much larger gap on both Nb 3d bands than on the  $\Gamma$  band [4].

In conventional superconductors, the delocalization of vortex core bound states occurs gradually on the scale of  $H_{c2}$ , and the characteristic length scale is  $\xi(0) \simeq \sqrt{\Phi_0/2\pi H_{c2}}$ . It appears that in  $\text{NbSe}_2$  (and  $\text{MgB}_2$ ), there are two characteristic length scales for delocalization:  $\xi^*$  and  $\xi(0)$ . To see this, we focus on the low field region. For  $\text{NbSe}_2$ , both  $\kappa/T$  and  $C/T$  have been measured with high precision on the same crystals, thereby making a detailed comparison possible. Fig. 4a shows the comparison for fields below  $H_{c2}/10$ , where the two do not coincide:  $C/T$  increases abruptly above  $H_{c1}$  while  $\kappa/T$  grows slowly, in an activated way. This is consistent with the presence of localized states at very low fields as imaged by STM [6, 21]. Then this behavior gives way to a rapid increase of the thermal conductivity at fields above  $0.03 H_{c2}$ . This is a clear indication that the field scale associated with the delocalization of quasiparticles in  $\text{NbSe}_2$  is much smaller than  $H_{c2}$ .

In fact, we can scale the behavior of the low-field thermal conductivity of  $\text{NbSe}_2$  to that of  $\text{V}_3\text{Si}$  using  $H^* = H_{c2}/9$  (Fig. 4b). This is also seen clearly if we

plot the ratio of the thermal conductivity to the specific heat (Fig. 4c) which measures the degree of delocalization. The ratio is seen to have two regimes: a rapid increase below  $H^* \simeq H_{c2}/10$  and a slow one above. In summary, the second length scale associated with delocalization in  $\text{NbSe}_2$  is  $\xi^* \simeq \xi(0)/\sqrt{9} = \xi(0)/3$ . This is consistent and may explain naturally the shrinking of the vortex cores observed with increasing field in  $\text{NbSe}_2$  via muon spin rotation [9].

Considering that the upper critical field is related to the superconducting gap by  $H_{c2} \propto \Delta^2/v_F^2$  where  $v_F$  is the Fermi velocity, we estimate the gap to vary over the FS by a factor of 3 ( $\Delta^* \simeq \Delta_0/3$ ). (Note that we assume  $v_F$  to be constant which is supported by band structure calculations [5].) A variation of this order has been reported earlier from STM measurements [6], where the spread in  $\Delta$  was measured to be between 0.7 meV and 1.4 meV. Moreover, theoretical modelling of STM features associated with the vortex cores was found to necessitate an anisotropy in the gap of a factor of 3 [22].

Our results are consistent with dHvA measurements [15], which detect extended quasiparticle excitations deep in the vortex state of both  $\text{NbSe}_2$  and  $\text{V}_3\text{Si}$ . Indeed, the scattering rate of  $\text{NbSe}_2$  decreases more slowly with decreasing field below  $H_{c2}$  than in  $\text{V}_3\text{Si}$ . The origin of MBSC in  $\text{NbSe}_2$  may lie in the fact that the electron-phonon coupling constant  $\lambda_{e-ph}$  is smaller for the  $\Gamma$  band. Corcoran *et al.* have measured  $\lambda_{e-ph} = 0.3$  for the  $\Gamma$  band whereas they extract a value of  $\lambda_{e-ph} = 1.8$  from comparing the calculated and measured values of the specific heat [5]. This suggests that superconductivity originates in the Nb 3d bands and is induced onto the Se 4p  $\Gamma$  pocket.

In summary, measurements of heat transport in the vortex state of  $\text{NbSe}_2$  at very low temperatures reveal the existence of highly delocalized quasiparticles down to fields very close to  $H_{c1}$ . This is in striking contrast with what is expected in a *s*-wave superconductor where well-separated vortices should support only localized states, as is observed in  $\text{V}_3\text{Si}$ . We have identified two characteristic length scales that govern the destruction of superconductivity in  $\text{NbSe}_2$ : the usual one associated with  $H_{c2}$  and another one associated with a much smaller field  $H^* \simeq H_{c2}/9$ . We attribute this to multi-band superconductivity, whereby the gap on the pocket-like  $\Gamma$  band is approximately 3 times smaller than the gap on the other two Fermi surfaces.

We are grateful to H.-Y. Kee, Y.B. Kim, W.A. MacFarlane, K. Machida, A.G. Lebed and K.B. Shamokhin for stimulating discussions. We also wish to thank Saša Dukan for providing us with theoretical calculations. This work was supported by the Canadian Institute for Advanced Research and funded by NSERC of Canada.

---

[1] G. Binnig *et al.*, Phys. Rev. Lett. **45**, 1352 (1980).

[2] H.J. Choi *et al.*, Nature **418**, 758 (2002), and references therein.

[3] M.R. Eskildsen *et al.*, cond-mat/0207394 (2002).

[4] T. Yokoya *et al.*, Science **294**, 2518 (2001).

[5] R. Corcoran *et al.*, J. Phys.: Condens. Matter **6**, 4479 (1994).

[6] H.F. Hess *et al.*, Physica B **169**, 422 (1991).

[7] E. Boaknin *et al.*, Phys. Rev. Lett. **87**, 237001 (2001).

[8] J. Sonier *et al.*, Phys. Rev. Lett. **82**, 4914 (1999).

[9] J. Sonier *et al.*, Phys. Rev. Lett. **79**, 1742 (1997).

[10] K. Takita and K. Masuda, J. Low Temp. Phys. **58**, 127 (1985).

[11] K. Yasui and T. Kita, Phys. Rev. Lett. **83**, 4168 (1999).

[12] W.F. Vinen *et al.*, Physica (Amsterdam) **55A**, 94 (1971).

[13] S. Dukan *et al.*, Phys. Rev. B **66**, 014517 (2002).

[14] For V<sub>3</sub>Si,  $\kappa_N/T$  is taken to be  $L_0/\rho_0$ , from the Wiedemann-Franz law where  $L_0$  is the Sommerfeld value of the Lorenz number and  $\rho_0$  is extrapolated from the resistivity - above  $T_c$  - which obeys a  $T^2$  temperature dependence. We use  $H_{c2}(0) = 18.5$  T as measured by Janssen *et al.* on the same crystals used in this study [15].

[15] T.J.B.M. Janssen *et al.*, Phys. Rev. B **57**, 11698 (1998).

[16] M. Nohara *et al.*, J. Phys. Soc. Jpn. **68**, 1078 (1999).

[17] A.V. Sologubenko *et al.*, Phys. Rev. B **66**, 014504 (2002).

[18] F. Bouquet *et al.*, cond-mat/0207141 (2002).

[19] A.P. Ramirez, Phys. Lett. A **211**, 59 (1996).

[20] G.R. Stewart and B.L. Brandt, Phys. Rev. B **29**, 3908 (1984).

[21] H.F. Hess *et al.*, Phys. Rev. Lett. **62**, 214 (1989).

[22] N. Hayashi *et al.*, Phys. Rev. Lett. **77**, 4074 (1996).

[23] It should be noted however that having such a similar behavior of the thermal conductivity and the specific heat is not what is expected for either a MBSC or a superconductor with an anisotropic gap in the case of superconductors in the clean regime (relevant for our crystals) as suggested by calculations of H. Kusunose *et al.*, cond-mat/0208113 (2002).